

Chapter 2

Unsolved Problems and Still-Emerging Concepts in Fractal Geometry

Benoit B. Mandelbrot

The preceding chapter sketches a striking property of fractal geometry. Its first steps are, both literally and demonstrably, childishly easy. But high rewards are found just beyond those early steps. In particular, forbiddingly difficult research frontiers are so very close to the first steps as to be understood with only limited preparation. Evidence of this unique aspect of fractal geometry is known widely, but scattered among very diverse fields. It is good, therefore, to bring a few together. A fuller awareness of their existence is bound to influence many individuals' and institutions' perception of the methods, goals, and advancements of fractal geometry.

1 Introduction

“You find fractals easy? This is marvelous.” Thus begins my response to an observation that is sometimes heard. “If you are a research mathematician, the community needs you to solve the challenging problems in this nice long list I carry around. If you are a research scientist, you could help to better analyze the important natural phenomena in this other long list.”

The first half-answer is elaborated in Section 2. The point is that fractal geometry has naturally led to a number of compelling mathematical conjectures. Some took 5, 10, or 20 years to prove, others—despite the investment of enormous efforts—remain open and notorious. If anything, what slows down the growth of fractal-based mathematics is the sheer difficulty of some of its more attractive and natural portions.

The second-half answer is elaborated in Section 3. The point is that, among other features, fractal geometry is, so far, the only available language for the study of roughness, a concept that is basic and related to our senses, but has been the last to give rise to a science. In many diverse pre-scientific

fields, the absence of a suitable language delays the moment when some basic problems could be attacked scientifically. In other instances, it even delays the moment when those problems could be stated.

2 From simple visual observation to forbiddingly difficult mathematical conjecture

A resolutely purist extreme view of art holds that great achievements must be judged for themselves, irrespective of their period and the temporary failures that preceded their being perfected. In contrast, the most popular view attaches great weight to cultural context and mutual influences, and more generally tightly links the process and its end-products. Some works do not survive as being excellent but as being representative or historically important. For example, a resolutely sociological extreme view that we do not share holds that Beethoven's greatness in his time and ours distracts from the more important appreciation of his contemporaries. Few persons, and not even all teachers, are aware that a very similar conflict of views exists in mathematics.

As widely advertised, the key product of mathematics consists in theorems; in each, assumptions and conclusions are linked by a proof. It is also well known that many theorems began in the incomplete status of conjectures that include assumptions and conclusions but lack a proof. The iconic example was a conjecture in number theory due to Fermat. After a record-breaking long time it led to a theorem by Wiles. Conjectures that resist repeated attempts at a proof acquire an important role, in fact, a very peculiar one. On occasion the news that an actual proof has made a conjecture into a theo-

rem is perceived as a letdown, while it is suggested that these conjectures' main value resides in the insights provided by both the unsuccessful and the successful searches for a proof.

Be that as it may, fractal geometry is rich in open conjectures that are easy to understand, yet represent deep mathematics. First, they did not arise from earlier mathematics, but in the course of practical investigations into diverse natural sciences, some of them old and well established, others newly revived, and a few altogether new. Second, they originate in careful inspections of actual pictures generated by computers. Third, they involve in essential fashion the century-old mathematical *monster shapes* that were for a long time guaranteed to lack any contact with the real world. Those fractal conjectures attracted very wide attention in the professions but elude proof. We feel very strongly that those fractal conjectures should not be reserved for the specialists, but should be presented to the class whenever possible. The earlier, the better. To dispel the notion that all of mathematics was done centuries ago, nothing beats being able to understand appropriate problems no one knows how to solve. Not all famous unsolved problems will work here: the Poincaré conjecture cannot be explained to high school students in an hour or a few. But many open fractal conjectures can.

For the reasons listed above, the questions raised in this chapter bear on an issue of great consequence. Does pure (or purified) mathematics exist as an autonomous discipline, one that can and should develop in total isolation from sensations and the material world? Or, to the contrary, is the existence of totally pure mathematics a myth?

The role of visual and tactile sensations. The ideal of pure mathematics is associated with the great Greek philosopher Plato (427?–347 BC). This (at best) mediocre mathematician used his great influence to free mathematics from the pernicious effects of the real world and of sensations. This position was contradicted by Archimedes (287–212 BC), whose realism I try to emulate.

Indeed, my work is unabashedly dominated by awareness of the importance of the messages of our senses. Fractal geometry is best identified in the study of the notion of roughness. More specifically, it allows a place of honor to full-fledged pictures that are as detailed as possible and go well beyond mere sketches and diagrams. Their original goal was modest: to gain acceptance for ideas and theories that were developed without pictures but were slow to be accepted because of cultural gaps between fields of science and mathematics. But those pictures then went on to help me and many others generate new ideas and theories. Many of these pictures strike everyone as being of exceptional and totally unexpected beauty. Some have the beauty of the mountains and clouds they are meant to represent; others are abstract and seem wild and unexpected at first, but after brief inspection appear totally familiar. In front of our eyes, the visual geometric intuition built on the practice of Euclid and of calculus is being retrained with the help of new technology.

Pondering these pictures proves central to a different philosophical issue. Does the beauty of these mathematical pictures relate to the beauty that a mathematician rooted in the twentieth century mainstream sees in his trade after long and strenuous practice?

2.1 Brownian clusters: fractal islands

The first example, introduced in Mandelbrot (1982), is a wrinkle on Brownian motion. The historical origins of random walk (drunkard's progress) and Brownian motion are known and easy to understand, at least qualitatively. From this, it is simple to motivate the definition of the Wiener Brownian motion: a random process $B(t)$ with increments $B(t+h) - B(t)$ that obey the Gaussian distribution of mean 0 and variance h , and that are independent over disjoint intervals.

For a given time L , the *Brownian bridge* $B_{\text{bridge}}(t)$ is defined by

$$B_{\text{bridge}}(t) = B(t) - (t/L)B(L),$$

for $0 \leq t \leq L$. Taking $B(0) = 0$, we find $B_{\text{bridge}}(L) = B_{\text{bridge}}(0)$. Combining one Brownian bridge in the x -direction and one in the y -direction and erasing time yields a *Brownian plane cluster* Q . Because we use Brownian bridges to construct it, the Brownian plane cluster is a closed curve. See Figure 1. An example of a well-known and fully proven

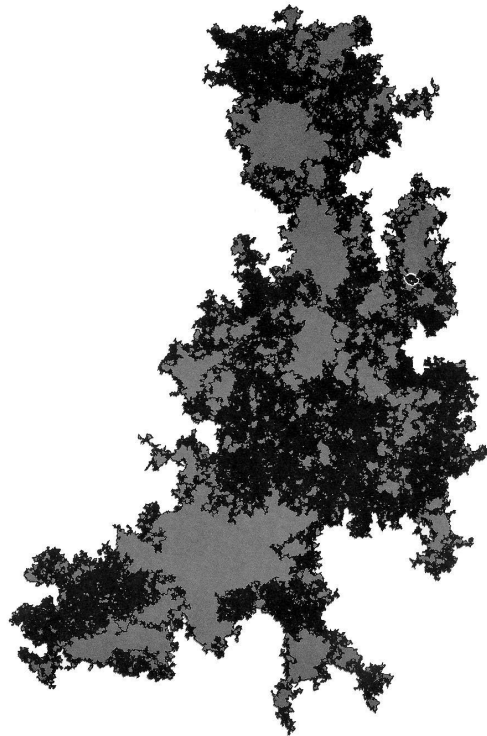


Figure 1: A Brownian plane cluster; Plate 243 of Mandelbrot (1982).

fact is that the fractal dimension of Q is $D = 2$. This result is important but not really perspicuous, because the big holes seem to contradict the association of $D = 2$ with plane-filling curves. Results that are well known and not perspicuous are not for the beginner.

Let us proceed to the *self-avoiding planar Brownian motion* \tilde{Q} . It is defined in Mandelbrot (1982) as the set of points of the cluster Q accessible from infinity by a path that fails to intersect Q . That is, \tilde{Q} is the *hull* of Q , also called its *boundary* or *outer edge*. The hull \tilde{Q} is easy to comprehend because it lacks double points. The unanswered question associated with it is the **4/3 Conjecture**, that \tilde{Q} has fractal dimension $4/3$.

An early example of Q , and hence of \tilde{Q} is seen in Figure 1. It looks like an island with an especially wiggly coastline, and experience suggested its dimension is approximately $4/3$. This comparison with islands made the $4/3$ conjecture sensible and plausible in 1982 and it remains sensible and plausible to students; that it remained a conjecture for many years is something they can appreciate. Numerical tests and physicists' heuristics were added to the empirical evidence and the conjecture was proved in Lawler, Werner, & Schramm (2000).

2.2 The Mandelbrot set

Second example: In the past, music could be both popular and learned, but *elitists* believe that this is impossible today. For mathematics, the issue was not raised because no part of it could be called a part of popular culture. Providing a counterexample, no other modern mathematical object has become part of both scientific and popular culture as rapidly and thoroughly as the Mandelbrot set. Moreover, an algorithm for generating this set is readily mastered by anyone familiar with elementary algebra. Thousands of people, from middle school children to senior researchers and Fields Medalists, have written programs to visualize various aspects of the Mandelbrot set.

Recall the simplest algorithm: a complex number c belongs to the Mandelbrot set M if and only if the sequence z_0, z_1, z_2, \dots stays bounded, where $z_0 = 0$ and $z_{i+1} = z_i^2 + c$.

For instance, the sequence can stay bounded by converging to a fixed point or to a cycle. Denote by M_0 the set of all c for which this is true. Of course, $M_0 \subset M$. In fact, M_0 is of interest to the students of dynamics, hence my original investigations were of M_0 , not of M . Interest shifted to M because producing pictures of M is easy. By contrast, to test if $c \in M_0$, we first generate several hundred or thousand points of the sequence z_0, z_1, z_2, \dots , and test if for large enough i there is an n for which $|z_{i+n} - z_i|$ is very small. This suggests convergence to a cycle of length n . (An impractical theoretical alternative is to solve the 2^n -degree polynomial equation $f_c^n(z) = z$, where $f_c(z) = z^2 + c$, then test the stability of the n -cycle by a derivative condition:

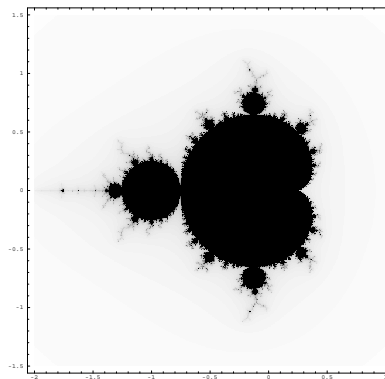


Figure 2: The Mandelbrot set.

$1 > |f'_c(w_1) \cdots f'_c(w_n)| = 2^n \cdot |w_1 \cdots w_n|$. Here the points w_1, \dots, w_n of the n -cycles are the sequences of successive z_i for different z_0 . In general, for each c there are several n -cycles, but at most one is stable.)

Computer approximations of M_0 actually yield a set smaller than M_0 , and computer approximations of M actually yield a set larger than M . Extending the duration of the computation seemed to make the two representations converge to each other and to an increasingly elaborate common limit. Furthermore, when c is an interior point of M , not too close to the boundary, it was easily checked that a finite limit cycle exists: the steps outlined above converge fairly rapidly for c not too close to the boundary. Those observations led me to conjecture that M is identical to M_0 together with its limits points, that is, $M = cl(M_0)$, the closure of M_0 .

In terms of its being simple and understandable without any special preparation, this conjecture is difficult to top. But after almost twenty years of study, it remains a conjecture. With the proof of Fermat's last theorem, the conjecture $M = cl(M_0)$ may have been promoted to illustrating the shortest distance between a simple idea (in this case, complete with popular pictures) and deep, unsolved mathematics. (Not so simple is the usual restatement of this conjecture: that M is locally connected.)

2.3 Dimensions of self-affine sets

The first tool for quantifying self-similar fractals is dimension. For a fractal consisting of N pieces, each scaled in all directions by a factor of r , the dimension D is given by

$$D = \frac{\log(N)}{\log\left(\frac{1}{r}\right)}.$$

This is easy to motivate, trivial to compute. Working through several examples, students soon develop intuition for the visual signatures of low- and high-dimensional fractals. The generalization to self-similar fractals having different scal-

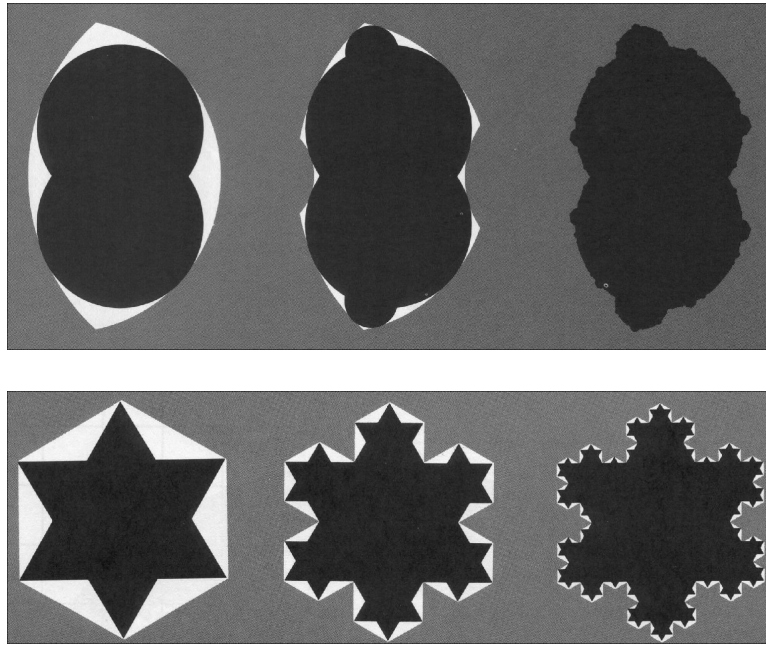


Figure 3: Top: Osculating circles outlining a Jordan curve limit set from inside and outside, Plate 177 of Mandelbrot (1982). Bottom: Osculating triangles outlining the Koch snowflake curve from inside and outside, Plate 43 of Mandelbrot (1982).

ings for different pieces is not difficult. For a fractal consisting of N pieces, the i^{th} piece scaled by a factor of r_i , the dimension D is the unique solution of the *Moran equation*

$$\sum_{i=1}^N r_i^D = 1.$$

Often this must be solved numerically, but this is not a difficulty given today's graphing calculators and computer algebra packages.

The simplicity of these calculations leads some people to believe that calculating dimensions is a simple process. This is a misperception resulting from the almost exclusive reliance on self-similar fractals for examples. The case of self-affine fractals, where the pieces are scaled by different factors in different directions, is much more difficult. Although some special cases are known, no simple variant of the Moran equation has been found. Kenneth Falconer describes the situation this way, "Obtaining a dimension formula for general self-affine sets is an intractable problem." (Falconer (1990), 129.) By simply changing the scaling factors in one direction, a completely straightforward exercise becomes tremendously difficult, perhaps without general solution.

2.4 Limit sets of Kleinian groups

A collection of Möbius transformations of the form $z \rightarrow (az + b)/(cz + d)$ defines a group that Poincaré called Kleinian. With few exceptions, their limit sets S are frac-

tal. For the closely related groups based on geometric inversions in a collection C_1, C_2, \dots, C_n of circles, there is a well-known algorithm that yields S in the limit. But it converges with excruciating slowness as seen in Plate 173 of Mandelbrot (1982). For a century, the challenge to obtain a fast algorithm remained unanswered, but it was met in many cases in Chapter 18 of Mandelbrot (1982). See also Mandelbrot (1983). In the case of this construction, fractal geometry did not open a new mathematical problem, but helped close a *very old* one.

In the new algorithm, the limit set of the group of transformations generated by inversions is specified by covering the complement of S by a denumerable collection of circles that *osculate* S . The circles' radii decrease rapidly, therefore their union outlines S very efficiently.

When S is a Jordan curve (as on Plate 177 of Mandelbrot (1982)), two collections of osculating circles outline S , respectively from the inside and the outside. They are closely reminiscent of the collection of osculating triangles that outline Koch's snowflake curve from both sides (Figure 3). Because of this analogy, the osculating construction seems, after the fact, to be very natural. But the hundred year gap before it was discovered shows it was not obvious. It came only after respectful examination of pictures of many special examples.

A particularly striking example is seen in Figure 4, called "Pharaoh's breastplate," Ken Monks' improved rendering of Plate 199 of Mandelbrot (1982). A more elaborate version of this picture appears on the cover of Mandelbrot (1999). This is the limit set of a group generated by inversion in the six

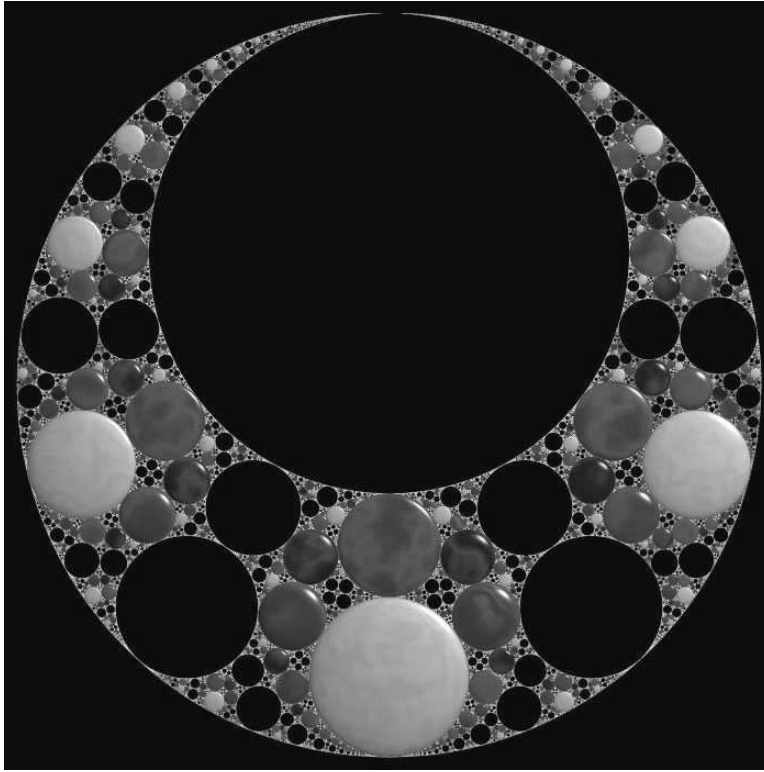


Figure 4: Left: Pharaoh’s breastplate. See the color plates. Right: the six circles generating Pharaoh’s breastplate, together with a few circles of the breastplate for reference.

circles drawn as thin lines on the small accompanying diagram. Here, the basic osculating circles actually belong to the limit set and do not intersect (each is the limit set of a Fuchsian subgroup based on three circles). The other osculating circles follow by all sequences of inversions in the six generators, meaning that each osculator generates a *clan* with its own *tartan* color.

By inspection, it is easy to see that this group also has three additional Fuchsian subgroups, each made of four generators and contributing full circles to the limit set.

Pictures such as Figure 4 are not only aesthetically pleasing, but they breathe new life into the study of Kleinian groups. Thurston’s work on hyperbolic geometry and 3-manifolds opens up the possibility for limit sets of Kleinian group actions to play a role in the attempts to classify 3-manifolds. The Hausdorff dimension of these limit sets has been studied for some time by Bishop, Canary, Jones, Sullivan, Tukia, and others. The group G that generates the limit set gives rise to another invariant, the *Poincaré exponent*

$$\delta(G) = \inf \left\{ s : \sum_{g \in G} \exp(-s\rho(0, g(0))) \right\} < \infty$$

where ρ is the hyperbolic metric. Under fairly general conditions, the Poincaré exponent of a Kleinian group equals the

Hausdorff dimension of the limit set of the group. See Bishop & Jones (1997), for example.

This is an active area of research: much remains to be done.

3 “Mathematics is a language”: the emergence of new concepts

History tells us that the great Josiah Willard Gibbs (1839–1903) made this remark at a Yale College Faculty meeting devoted to the reform of foreign language requirements (some faculty issues never die!). The context may seem undignified or amusing, but, in fact, Gibbs’s words bring forth a deep issue. To express subtle scientific ideas, one often needs new *words* that are subtler than those of ordinary language.

As background, everyone knows that some great books deservedly became classics because they provided, for the first time, a new language in which personal emotions—that the reader would feel but not be able to express—could be both refined and made public. This is not at all a matter of coining new words for old concepts but of making altogether new concepts emerge.

Advances in the sciences are assessed in diverse ways, one of which is the emergence of new scientific concepts. Indeed, the facile precept that the first step is to observe then measure,

sounds less compelling when the object of study is an undecipherable mess and all the measurements that readily come to mind disagree or even seem self-contradictory. This is why the point of passage from prescientific to scientific investigation is often marked by what Thomas Kuhn called *change of paradigm*. Sometimes this includes the appearance of a suitable new language, without which observations could not be made and quantified.

3.1 Fractals are a suitable language for the study of roughness wherever it is encountered

Let us ponder the ubiquity of the notion of roughness and its lateness in becoming formalized. Many sciences arose directly from the desire to describe and understand some basic messages the brain receives from the senses. Visual signals led to the notions of bulk and shape and of brightness and color. The sense of heavy versus light led to mechanics and the sense of hot versus cold led to the theory of heat. Other signals (for example, auditory) require no comment. Proper measures of mass and size go back to prehistory and temperature, a proper measure of hotness, dates to Galileo.

Against this background, the sense of smooth versus rough suffered from a level of neglect that is noteworthy though hardly ever pointed out. Not only does the theory of heat have no parallel in a theory of roughness, but temperature itself had no parallel until the advent of fractal geometry. For example, in the context of metal fractures, roughness was widely measured by a root mean square deviation from an interpolating plane. In other words, metallurgists used the same tool as finance experts used to measure volatility. But this measurement is inconsistent. Indeed, different regions of a presumably homogeneous fracture emerged as being of different r.m.s. volatility. The same was the case for different samples that were carefully prepared and later broken following precisely identical protocols.

To the contrary, as shown in Mandelbrot, Passoja & Paullay (1984) and confirmed by every later study, the fractal dimension D , a characteristic of fractals, provides the desired invariant measure of roughness. The quantity $3 - D$ is called the codimension or Hölder exponent by mathematicians and now called the roughness exponent by metallurgists.

The role played by exponents must be sketched here. It is best in this chapter to study surfaces through their intersections by approximating orthogonal planes. Had these functions been differentiable, they could be studied through the derivative defined by $P'(t) = \lim_{\epsilon \rightarrow 0} (1/\epsilon)[P(t + \epsilon) - P(t)]$. For fractal functions, however, this limit does not exist and the local behavior is, instead, studied through the parameters of a relation of the form $dP \sim F(t)(dt)^\alpha$. Here $F(t)$ is called the prefactor, but the most important parameter is the exponent $\alpha = \lim_{\epsilon \rightarrow 0} \{\log[P(t + \epsilon) - P(t)] / \log \epsilon\}$.

There is an adage that, when you own only a hammer, everything begins to look like a nail. This adage does not apply to roughness.

3.2 Fractals and multifractals in finance

Versions of the Brownian motion model mentioned in Section 2.1 are widely used to model aspects of financial markets. In fact, and contrary to common belief, the first analysis of Brownian motion was not advanced in 1905 by Einstein. In 1900 Bachelier had already developed Brownian motion to study the stock market.

Despite this historical precedent, successive differences of real data sampled at equal time intervals reveal even on cursory investigation that Brownian models are very far from being tolerable. Most visibly, (1) the width of the *central band* is not constant, but varies substantially, (2) the excursions from the central band are so large as to be astronomically unlikely in the Brownian case, and (3) the excursions are not independent, but occur in clumps, often when the underlying band is widest. Figure 5 illustrates these differences.

Ad hoc fixes can account for each of these failures of the Brownian model, but very rapidly become far too complicated for anybody, especially for courses not addressed to experts. The fractal/multifractal approach of Mandelbrot (1997) is much more elegant. It provides a unified way to synthesize all, and moreover introduces a family of parameterized cartoon models suitable for student exploration.

Let us dwell on what is happening. Compared with well-developed standard mathematical finance, the fractal cartoons are incomparably more satisfactory. But they are far simpler than the first stages of standard finance, so simple that they have been immediately incorporated into both *Fractal Geometry for Non-Science Students* (a course primarily for humanities students) and *Fractal Geometry: Techniques and Applications* (a course for sophomore-junior math and science students) at Yale. In effect, students are invited to participate in discussions between experts. They are amazed by the realistic appearance of forgeries made with these cartoons. Showing the class a collection of real data and forgeries always produces interesting results. Students disagree, sometimes with great animation, about which are real and which are forgeries. The *inverse problem*, finding a cartoon to create a forgery of a particular data set, has been a source of interesting student projects, some quite creative. After studying background in the different visual signatures of long tails and global dependence, students are amazed at how slight changes in the cartoon generator can achieve both effects.

The basic construction of the cartoon involves an *initiator* and a *generator*. The process to be iterated consists of replacing each copy of the initiator with an appropriately rescaled copy of the generator. For a first cartoon, the initiator is the diagonal of the unit square, and the generator is the broken line with vertices $(0, 0)$, $(4/9, 2/3)$, $(5/9, 1/3)$, and $(1, 1)$. Fig-



Figure 5: Left: differences in successive daily closing prices for four years of EMC data. Right: successive differences of the same number of steps in one-dimensional Brownian motion.

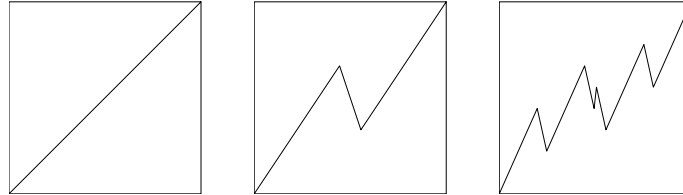


Figure 6: The initiator, generator, and first iterate of a non-random Brownian motion cartoon.

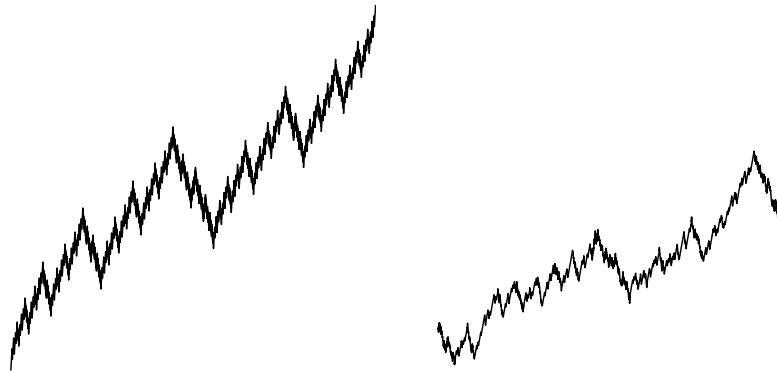


Figure 7: Left: the 6th iterate of a non-random Brownian cartoon. Right: the 6th iterate of a randomized Brownian cartoon.

Figure 6 shows the initiator (left), generator (middle), and first iteration of the process (right).

To get an appreciation for how quickly the jaggedness of these cartoons grows, the left side of Figure 7 shows the 6th iterate of the process.

Self-affinity is guaranteed because it is built into the process; each piece is an appropriately scaled version of the whole. In this case, the scaling ratios have been selected to satisfy the square root condition of Brownian motion. The horizontal axis denotes time t , the vertical denotes price x . The first and third generator segments have $\Delta t_1 = \Delta t_3 = \frac{4}{9}$ and $\Delta x_1 = \Delta x_3 = \frac{2}{3}$; the middle segment has $\Delta t_2 = \frac{1}{9}$ and $\Delta x_2 = -\frac{1}{3}$. So for each generator segment we have $|\Delta x_i| = (\Delta t_i)^{1/2}$.

A cartoon is *unifractal* if there is a constant H so that for each generator segment $|\Delta x_i| = (\Delta t_i)^H$. If different H are needed for different segments, the cartoon is *multifractal*.

The left side of Figure 7 is far too regular to mimic any real data. But it can be randomized easily by shuffling the order in which the three pieces of the generator are put into each

scaled copy. The right side of Figure 7 shows the result of this shuffling, for the sixth stage of the construction.

Instead of the graph itself, it is less common but far better to look at the increments. The cartoon sequence we have produced has jumps at uneven intervals: some at multiples of $1/3^n$, some at multiples of $1/9^n$. Because we rarely have detailed knowledge of the underlying dynamics generating real data, measurements usually are taken at equal time steps. To construct a sequence of appropriate increments, we sample the graph at fixed time intervals and subtract successive values obtained. Operationally, first make a list of time values for the sampling, then find the cartoon time values between which each sample value lies, and linearly interpolate between the cartoon values to find the sample value at the sample time.

Figure 8 illustrates how the statistical properties of the differences can be modified by making a simple adjustment in the generator. Fixing the points $(0, 0)$ and $(1, 1)$, we keep the middle turning points symmetrical: $(a, \frac{2}{3})$ and $(1 - a, \frac{1}{3})$, where a lies in the range $0 < a \leq \frac{1}{2}$. All pictures were constructed from the tenth generation, hence consist of $3^{10} =$

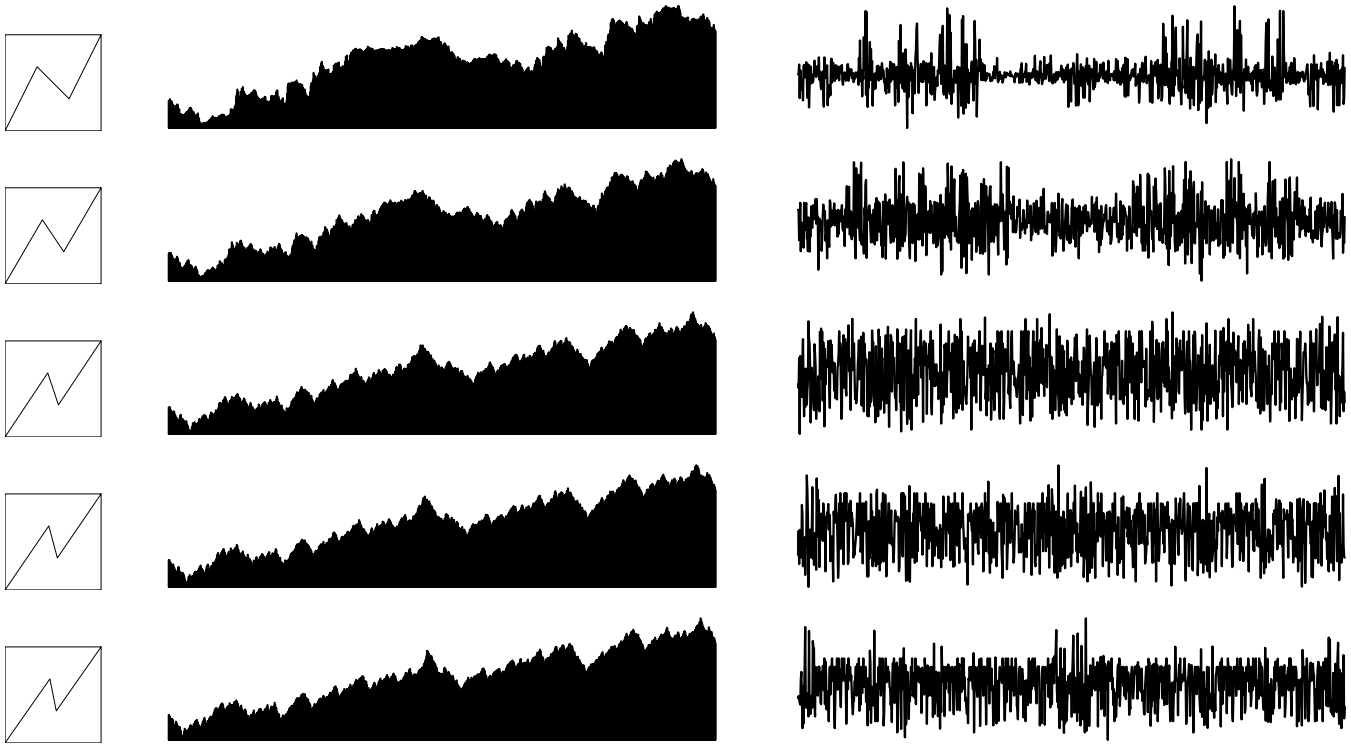


Figure 8: Generators, cartoons and difference graphs for symmetric cartoons with turning points $(a, \frac{2}{3})$ and $(1 - a, \frac{1}{3})$, for $a = 0.333, 0.389, 0.444, 0.456, \text{ and } 0.467$. The same random number seed is used in all graphs.

59,049 intervals. The difference graphs are constructed by sampling at 1000 equal time steps.

Certainly, correlations are introduced as the point $(4/9, 2/3)$ is moved to the left. Of course, this is just the beginning. More detailed study reveals relations between the Hölder exponents and the slopes of the generator intervals, and properties of the multifractal measure can be extracted from the cartoons (Mandelbrot (1997)). The H -exponents and the $f(\alpha)$ curve are much too technical for *Fractal Geometry for Non-Science Students*, but are appropriate topics for the more mathematically sophisticated *Fractal Geometry: Techniques and Applications*. Even for this audience, these are challenging concepts. Yet these simple cartoons provide accessible introductions to some of the subtle mathematics of multifractals.

As a last example, we mention a fascinating theorem and a visual representation of its meaning. The Yale students taking *Fractal Geometry for Non-Science Students* in autumn of 1998 followed the development of Figure 9 with passion and helped improve it. The generator increments Δt represent *clock time*. Viewed in clock time, prices sometimes remain quiescent for long periods, and sometimes change with startling rapidity, perhaps even discontinuously. For these cartoons, clock time can be recalibrated to uniformize these changes in price variation. Basically, slow the clock during periods of rapid activ-

ity and speed it during periods of low activity. Students found the VCR a useful analog. Fast-forward through the commercials (low activity) and use slow-motion through the interesting bits (rapid activity).

For the cartoon generators, this is achieved by first finding the unique solution D of $|\Delta x_1|^D + \dots + |\Delta x_n|^D = 1$, then defining the *trading time* generators by $\Delta T_i = |\Delta x_i|^D$. By changing to trading time, every multifractal price cartoon can be converted into a unifractal cartoon in multifractal time. Global dependence and long tails are unpacked in different ways by converting to trading time. Specifically, global dependence remains in the price vs. trading time record, but the long tails are absorbed into the multifractal nature of trading time.

Figure 9 shows a three-dimensional representation of this conversion. Note how the clock time-trading time curve compresses the flat regions and expands the steep regions of the price-clock time graph. Thus the long tails of the price-clock time graph are absorbed into the multifractal time measure. In addition, the dependence of increments is uniformized to fractional Brownian motion in the price-trading time graph. That is, the conversion to trading time decomposes long tails and dependent increments into different aspects of the graph.

Starting from a rough idea of such a representation, this picture evolved over about a week, through discussions with the class. Few things have excited the class as much as being

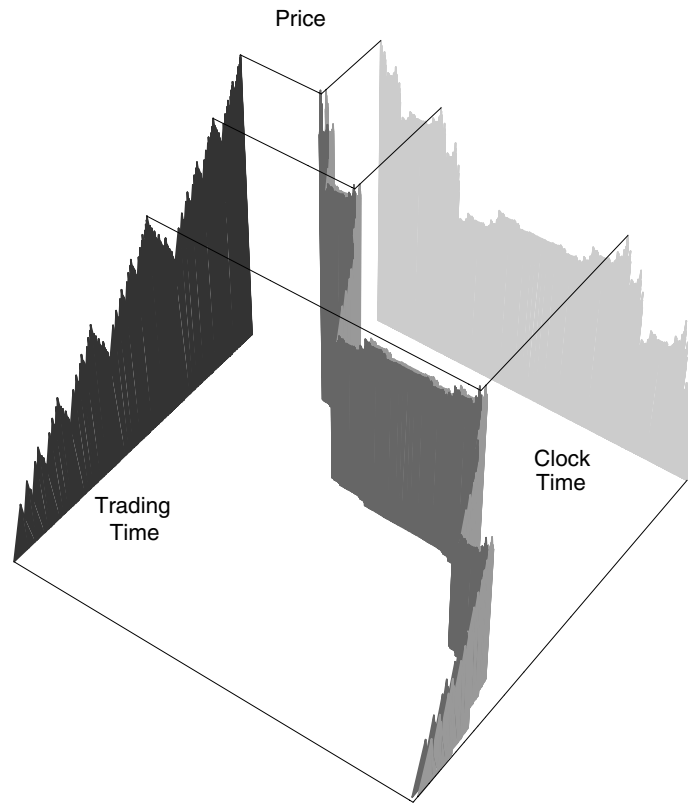


Figure 9: Converting the price-clock time graph to the price-trading time graph by means of the clock time-trading time graph.

involved, as a group, in the production of a figure to explain current research in the field.

4 Conclusion

A famous tongue-twister and test in Greek and evolution, due to E. H. Haeckel, proclaims that “ontogeny recapitulates phy-

logeny.” In plainer English, the early growth of an individual repeats the evolution of its (his, her) ancestors. As argued elsewhere in this book (Chapter 3), this used to be the **BIG PICTURE** historical justification of *old math*—not a well-documented one. But teachers ought to welcome any well-documented **small picture** version that happens to come their way. Fractals deserve to be welcomed.

